PLANT SCIENCE TODAY
Vol 13(1): 1-9
https://doi.org/10.14719/pst.11901

eISSN 2348-1900

RESEARCH ARTICLE

# Characterization and detoxification of foot patch by gelatin-agar-based phase hydrogel

**Sonam Ahuja[1]*, Vijay Jagdish Upadhye[2], Malek Moinhusain Inayat Koderbhai[1], Patel Jahnvi Samirbhai[1], Bariya Jaydeepkumar Ramsingbhai[1], Sangani Yash Nimeshbhai[1], Srushtirajsinh Rana[1], Hardikkumar Satishbhai Chauhan[1], Nikhilkumar Dipakbhai Padhiyar[1] & Patel Janvi Dilipbhai[1]**

[1]Department of Chemical Science, Parul Institute of Applied Science, Parul University, Vadodara 391 760, Gujrat, India
[2]Research and Development Cell, Department of Microbiology, Parul Institute of Applied Science, Parul University, Vadodara 391 760, Gujrat, India

*Correspondence email - sonam.ahuja82106@paruluniversity.ac.in

Received: 22 September 2025; Accepted: 03 December 2025; Available online: Version 1.0: 29 January 2026; Version 2.0: 05 February 2026

**Cite this article:** Sonam A, Vijay JU, Malek MIK, Patel JS, Bariya JR, Sangani YN, Srushtirajsinh R, Hardikkumar SC, Nikhilkumar DP, Patel JD. Characterization and detoxification of foot patch by gelatin-agar-based phase hydrogel. Plant Science Today. 2026; 13(1): 1-9. https://doi.org/10.14719/pst.11901

## Abstract

Hydrogels made of gelatin and agar have attracted considerable interest for a multitude of pharmaceutical and biomedical applications due to their biodegradability, biocompatibility and controlled release of bioactive materials. These biopolymers include gelatin, a protein derived from collagen and agar, a polysaccharide obtained from red algae; they are used synergistically to manufacture hydrogels with improved mechanical and swelling properties. Investigation of the properties of these hydrogels is essential for describing their structure and function. Infrared Spectroscopy, particularly Fourier Transform Infrared Spectroscopy (FTIR), is commonly used to detect functional groups in the hydrogel matrix. Secondary electron imaging by Scanning Electron Microscopy (SEM) is used in determining the topographical images of the hydrogels. The thermal stability of the hydrogels is determined by conducting Thermo Gravimetric Analysis (TGA). Ultraviolet-Visible (UV-Vis) Spectroscopy is used to determine the extent of L-ascorbic acid immobilization in the hydrogel network. The absorption spectra can identify the drug at those wavelengths and determine the drug loading and release profile in the hydrogel system. This study aimed to develop and characterize gelatin-agar-based hydrogels for potential drug delivery applications, highlighting their structural, thermal and functional properties through comprehensive physicochemical analyses.

**Keywords:** agar powder; anti-inflammatory properties; anti-microbial properties; bovine albumin; detoxification; gelatine polymer; glutaraldehyde; human blood; hydrochloric acid; L-ascorbic acid

## Introduction

In recent years, particular attention has been paid to the behaviour of co-hydrogels. A composite hydrogel is a network of two or more polymers that are cross-linked (1, 2). Therefore, altering the co-hydrogel or composite composition can control their properties (3). Because gelatin and agar are both biocompatible, gelatin–agar co-hydrogels have attracted considerable interest for the long-term release of bioactive molecules. Agar and gelatin are characterized as naturally occurring polymers. Collagen is partially hydrolyzed to produce gelatin, a protein widely used in food processing. Additionally, gelatin and agar are readily available and reasonably priced (4, 5). Phase separation in hydrogels occurs because systems containing gelatin and polysaccharides in solution exhibit thermodynamic instability at high concentrations of both gelatin and polysaccharides (6). The hardened gels that form after cooling the hot trap containing the gelatin–polysaccharide mixtures are water-in-water emulsions. In these emulsions, the internal phase contains a polysaccharide, while the outer phase is gelatinous. Because of their structural and compositional similarities to the extracellular matrix (ECM), hydrogels are materials with a wide range of applications in the pharmaceutical and biomedical industries. Over the past few decades, numerous hydrogel types with various chemical and physical characteristics have been created using both natural and synthetic water-soluble polymers, including cellulose, hyaluronic acid, fibrin, chitosan and agar, as well as synthetic polymers like poly(acrylic acids), poly(acrylamides), poly(ethylene oxide), poly(vinyl alcohols) and poly(vinyl pyrrolidones) (7). They are three-dimensional crosslinked polymer chains that can entrap a large volume of water; thus, their applications are far-reaching in medical, environmental and industrial uses, among others. Two natural polymers commonly used to synthesize hydrogels are gelatin and agar, which differ in their characteristics because they are derived from natural sources. Gelatin was used for the following reasons: it is biocompatible and biodegradable, has a relatively high crosslinking capacity and is stable under physiological conditions (8). Further contributions of additional gelation and cross-linking properties of hydrogel solution to support the cells, along with providing thermo-stable hydrogel and also maintain the balance between easy melting of the hydrogel and good gel stability at relatively higher temperatures (9). This will also affect the electrical, thermal and chemical processes.

In light of the aforementioned, the current study aimed to develop a phase-separated hydrogel composed of gelatin and agar. Fourier Transform Infrared Spectroscopy (FTIR), Scanning Electron Microscopy (SEM), Thermo Gravimetric Analysis (TGA), mechanical and swelling index tests and electrical studies were used to thoroughly characterize the prepared formulations. Additionally, the formulations' drug-release characteristics and the impact of formulated swelling were assessed. Ultraviolet-Visible spectroscopy was used to characterize L-ascorbic acid, the model antimicrobial drug used in the drug-release studies.

## Materials and Methods

### Materials

Gelatin powder was purchased from TGP Bioplastics Pvt. Ltd, Satara, Maharashtra, India. Agar-agar powder, glutaraldehyde and hydrochloric acid (HCl) were also purchased from TGP Bioplastics Pvt. Ltd, Satara, Maharashtra, India. L-ascorbic acid was purchased from Parul University Vadodara, Gujarat, India. Bovine albumin was purchased from Chitu-Chem Corporation, Vadodara, Gujarat; fresh human blood was obtained from the hospital. Distilled water was used throughout the study.

### Preparation of hydrogels

Two grams of agar powder were mixed with 100 mL of water and autoclaved for 15 min at 15 atmospheres and 120 °C. As a result, a 2 % (w/w) agar solution formed. Twenty grams of gelatin powder was suspended in 70 mL of water to create a 20 % (w/w) gelatin solution. To dissolve the gelatin, the suspension was heated to 65 °C. Using hot water, the gelatin solution was brought to a final weight of 100 g. As a result, a 20 % (w/w) gelatin solution formed. Using an overhead stirrer, 15 g of agar solution and 5 g of gelatin solution were homogenized at 70 °C for 5 min (300 rpm). To crosslink the gelatin-agar matrix, 0.5 mL of glutaraldehyde reagent (0.5 mL glutaraldehyde + 0.5 mL ethanol + 0.1 mL 0.1 N HCl) was added for 10 sec, then poured into a Petri plate or beaker and left to stand at room temperature for 30 min (10). Table 1 provides a variety of hydrogel ratios.

**Table 1.** Composition of hydrogels

| S. No. | Gelatin (g) | Agar (g) |
|---|---|---|
| 1. | 10 | 10 |
| 2. | 12 | 8 |
| 3. | 8 | 12 |
| 4. | 15 | 5 |
| 5. | 5 | 15 |

### Preparation of drug-loaded hydrogel

L-ascorbic acid (1 % w/w) was dissolved in the gelatin-agar solution. After preparation optical image was observed (Fig. 1).

### Swelling study

Swelling investigations were conducted in the pseudo-extracellular fluid (PEF). The fluid's composition was as follows: 25 g of sodium (Na), 6.8 g of sodium chloride (NaCl), 2.2 g of potassium chloride (KCl), 3.5 g of sodium dihydrogen phosphate ($NaH_2PO_4$) and 3.5 g of sodium bicarbonate ($NaHCO_3$) in one liter. This solution's pH was determined to be 7.36. The pre-weighed hydrogel sample was submerged in 25 mL of PEF and removed at various time points. It was then thoroughly cleaned with tissue paper to eliminate any remaining surface water, weighed precisely in an electronic balance (Denber, Germany) and submerged in water once more. The following formula was used to determine the swelling ratio (SR) (11):

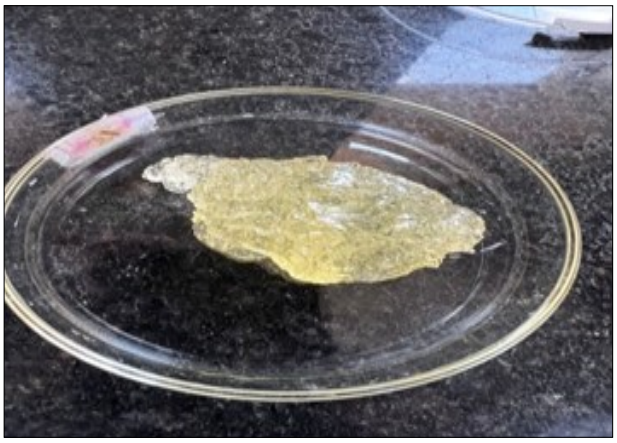

**Fig. 1.** Drug-loaded hydrogels.

$$\text{Swelling ratio} = \frac{W_t - W_i}{W_i} \times 100 \qquad \text{(Eqn. 1)}$$

Where, Wt and Wi are the initial weight and the weight in different time intervals weight of micropates after time t (Table 2).

**Table 2.** Different ratios of gelatin and agar hydrogels

| Time | Different ratios of gelatin and agar hydrogels | | | | |
|---|---|---|---|---|---|
| | G12:A8 | G8:A12 | G15:A5 | G5:A15 | G10:A10 |
| 00 min | 3.344 g | 2.068 g | 4.082 g | 1.709 g | 1.502 g |
| 30 min | 3.880 g | 2.394 g | 4.858 g | 2.218 g | 2.205 g |
| 60 min | 4.083 g | 2.583 g | 5.338 g | 2.442 g | 2.530 g |
| 90 min | 4.235 g | 2.660 g | 5.455 g | 2.655 g | 2.673 g |
| 120 min | 4.504 g | 2.860 g | 5.912 g | 2.812 g | 3.083 g |
| 150 min | 4.753 g | 3.035 g | 6.307 g | 2.976 g | 3.365 g |
| 180 min | 4.793 g | 3.064 g | 6.960 g | 2.999 g | 3.468 g |
| 24 hr | 8.892 g | 5.565 g | 9.749 g | 4.859 g | 6.258 g |

### Dynamics of moisture uptake

Using the described technique, a saturated potassium nitrate ($KNO_3$) solution was placed in a plastic jar and a rectangular block of stainless steel, with its top above the solution level, was placed in the centre of the jar to measure the kinetics of moisture uptake. The steel block was now topped with an aluminum crucible. The crucible was filled with a pre-weighed piece of perfectly dry film, the jar's lid was securely fastened and it was kept at 37 °C in an incubator. The film was removed at specified intervals, weighed precisely using an electronic balance (Denber, Germany) and then returned to the jar. The mass measurements were recorded as g/g and continued until equilibrium was reached (11):

$$\frac{1}{(m-m_0)} = \frac{1}{k(m_e-m_0)} + \frac{1}{(m_e-m_0)} \qquad \text{(Eqn. 2)}$$

Where, m is the mass of the hydrated film at various time intervals and $m_0$ and me are the masses of the dry and fully equilibrated film samples, respectively (Table 3).

### Antibacterial activity

The standard agar disc diffusion method was used to assess antibacterial activity against a few specific bacterial species. Three 100 mL of distilled water was used to suspend 3.9 g of nutrients and 7.5 g of agar powder, which were then autoclaved for 15 min at 121 °C and 15 atmospheric pressure (11). Following cooling, the media

**Table 3.** Moisture uptake data of the hydrogel

| Time (min) | G12:A8 | G8:A12 | G15:A5 | G5:A15 | G10:A10 |
|---|---|---|---|---|---|
| 0 | 0 | 0 | 0 | 0 | 0 |
| 15 | 0.178 | 0.096 | 0.074 | 0.073 | 0.084 |
| 30 | 0.240 | 0.211 | 0.097 | 0.077 | 0.092 |
| 45 | 0.299 | 0.231 | 0.144 | 0.124 | 0.111 |
| 60 | 0.401 | 0.256 | 0.211 | 0.169 | 0.134 |
| 75 | 0.412 | 0.301 | 0.234 | 0.174 | 0.158 |
| 90 | 0.463 | 0.310 | 0.240 | 0.181 | 0.177 |

were transferred into petri dishes and allowed to solidify for 30 min. Drug-loaded hydrogels were added to a single 50 µL fresh culture that had been spread on solidified nutrient agar plates. One is 100 mg $mL^{-1}$ and is incubated for 24 hr at 37 °C. The zone of inhibition growth was examined following a 24 hr incubation period. The microorganisms' susceptibility to the antimicrobial agent increases with the diameter of the inhibition zone (12).

## Anti-inflammatory activity

The albumin denaturation inhibition method was used to evaluate the *in vitro* anti-inflammatory properties of the synthesized compounds. To ensure that the final dimethyl formamide (DMF) concentration in all solutions remained less than 2.0 %, for the standard medication and the test compounds, the medication was first dissolved in a small portion of DMF and the solution was further diluted with 0.2 M phosphate buffer at pH 7.4. After mixing 1 mL of 1 % albumin solution in phosphate buffer with 1 mL of the test solution at various drug doses, the culture mixture was incubated in a biochemical oxygen demand (BOD) incubator for 15 min. After this, the prepared reaction mixture was heated in a water bath at 60±1 °C for 5-10 min to promote denaturation. The turbidity reading was taken at 660 nm. After cooling, denaturation was calculated using a non-medicated group of rabbits that served as the control animals. Each experiment was repeated three times and the average was later taken (13). The typical medication was diclofenac sodium. It demonstrates the percentage inhibitory effect of albumin denaturation, as listed in the table below. The percentage of inhibition of protein denaturation is calculated using the following formula (14) (Table 4).

$$\text{Inhibition (\%)} = \left( \frac{\text{Control OD - Sample OD}}{\text{Control OD}} \right) \times 100 \quad \text{(Eqn. 3)}$$

Where, OD is the optical density.

## Biocompatibility study

Haemo-compatibility was also used to test the formulations' biocompatibility. The degree of haemolysis upon contact with the samples is calculated to determine the hemocompatibility assessment. The leachants in the formulations were created using regular saline solution. The mixture contained 0.5 mL of leachant and 0.5 mL of human blood, which had been previously diluted with regular saline at a 4:5 ratio. Ten milliliters of wash solution were prepared using normal saline and 0.5 mL of 0.01 N solution was used for the positive and negative controls. In this study, 0.5 mL of saline and 1 mL of HCl were used as alternatives to the formulations. After mixing the test and control samples with 0.5 mL of human blood, the mixture was diluted with regular saline to a final volume of 10 mL. Following a 1 hr incubation period at 37 °C, the test samples and controls were spun for 10 min at 3000 rpm. Following centrifugation of the sample solutions, the supernatant was analysed using a Ultraviolet-Visible (UV-Vis) Spectroscopy set to 545 nm. The haemolysis percentage was determined using the following formula (15):

**Table 4.** Concentrations of L-ascorbic acid as anti-inflammatory agent

| Concentration (%) | Control (OD) | Sample (OD) | % Inhibition |
|---|---|---|---|
| 1 | 0.25 | 0.04 | 84.00 |
| 2 | 0.34 | 0.04 | 88.23 |
| 3 | 0.49 | 0.04 | 91.83 |
| 4 | 0.58 | 0.04 | 93.10 |
| 5 | 0.72 | 0.06 | 91.66 |

$$\text{Haemolysis (\%)} = \frac{\text{OD test - OD negative}}{\text{OD positive - OD negative}} \times 100 \quad \text{(Eqn. 4)}$$

Where, OD test is the absorbance in the test sample, OD positive is the absorbance in the positive control. OD negative is the absorbance with the negative control.

Haemolysis is done with two different hydrogels. One with a drug loaded and the second is without a drug loaded, as shown in table 5 and 6 (16).

## Characterization

Ultraviolet-Visible (UV-Vis) (Shimadzu, 1800) absorption spectrophotometry refers to the capability to quantify the decrease in the intensity of the electromagnetic radiation within a wavelength range of 190-800 nm and FTIR (Shimadzu, 8400, Japan) was used to record the FTIR spectra using potassium bromide (KBr). The powdered material was combined with KBr. The average of 100 scans, with a spectral range of 400-4000 $cm^{-1}$, was used. The X-ray diffractogram was captured at 2° $min^{-1}$ over the range of 3° to 50°. Scanning electron microscopic images were captured using a Hitachi S-4700 (New Jersey, USA) at an acceleration voltage of 15 kV to examine the surface morphology of the Starch/PVA film. Ultraviolet-Visible spectrophotometer is also used to determine the λ max. The characterization was carried out by the PNP Analytical Solutions Laboratory in Vadodara, Gujarat, India, which is important for understanding how the hydrogel will behave during processing and storage. During the analysis, all safety measures were considered to avoid any danger to participants (17-19).

**Table 5.** Haemolysis test of drug-loaded hydrogels

| Concentration | Absorbance 1 | Absorbance 2 | Absorbance 3 | Mean | % Haemolysis |
|---|---|---|---|---|---|
| 20 | 0.662 | 0.612 | 1.056 | 0.77667 | -282.288 |
| 40 | 0.647 | 0.921 | 0.987 | 0.85167 | -323.801 |
| 60 | 0.798 | 0.975 | 1.084 | 0.95233 | -379.520 |
| 80 | 0.497 | 0.220 | 0.701 | 0.47267 | -114.022 |
| 100 | 0.139 | 0.311 | 0.285 | 0.24500 | 11.9926 |

**Table 6.** Haemolysis test of without drug loading hydrogels

| Concentration | Absorbance 1 | Absorbance 2 | Absorbance 3 | Mean | % Haemolysis |
|---|---|---|---|---|---|
| 20 | 0.123 | 0.181 | 0.227 | 0.177 | 49.631 |
| 40 | 0.454 | 0.729 | 0.371 | 0.518 | -139.114 |
| 60 | 0.681 | 3.081 | 0.656 | 1.472 | -667.528 |
| 80 | 0.135 | 0.211 | 0.912 | 0.419 | -84.5018 |
| 100 | 0.465 | 0.277 | 1.197 | 0.646 | -210.148 |

## Results and Discussion

### Swelling study

To develop a swelling test for composite gels, 8.307 g of NaCl and 0.367 g of calcium chloride ($CaCl_2$) were dissolved in 1 L of distilled water to prepare the physiological fluid (PF) solution. All the gelatin-agar composite ratio gels, except the last set, were immersed in the PF solution. Swelling measurements were taken after 30 min and repeated 3-4 times, with an additional measurement after 24 hr. The PF swelling test is described with PF increasing with the weight of the hydrogel. Swelling experiments are used to compare the variations among different composite gels. Based on analysis of all gel ratios (8:8, 12:15, 5:15, 10), the dry weight of the 15:5 composite gel was found to be higher than that of the other composites (Fig. 2) (20).

### Ultraviolet Visible Spectroscopy

In the UV region (200-250 nm), the spectrum shows a high absorbance of approximately 4.0; beyond 300 nm, the absorbance rapidly drops to near zero (21). The rapid decline indicates that L-ascorbic acid has a strong affinity for UV radiation due to its conjugated system, or chromophore, which involves π-π* transitions. There is no significant absorbance in the visible region (>400 nm), consistent with the molecule being colourless (Fig. 3).

### Fourier Transform Infrared Spectroscopy

While most of the rays continue to pass through the material, some infrared photons are absorbed during FTIR analysis. The spectrum, which shows absorption or transmittance as a function of wavelength, is used to identify the sample substances. The transmittance of each of the three compounds was measured using FTIR in the range of 3500-1000 $cm^{-1}$. Fourier Transform Infrared Spectroscopy was subsequently used to characterize the by-product and the results are shown in the figure below. The peak at 3271.39 $cm^{-1}$, corresponding to the broad OH or acute NH stretching vibration of gelatin, showed a significant transmittance. At the summit, the C=O (ketones, carboxylic acids, amides) group stretching is observed as a peak at 1628.86 $cm^{-1}$ in the infrared spectrum of gelatin. Another peak was discovered at 1543.31 $cm^{-1}$,

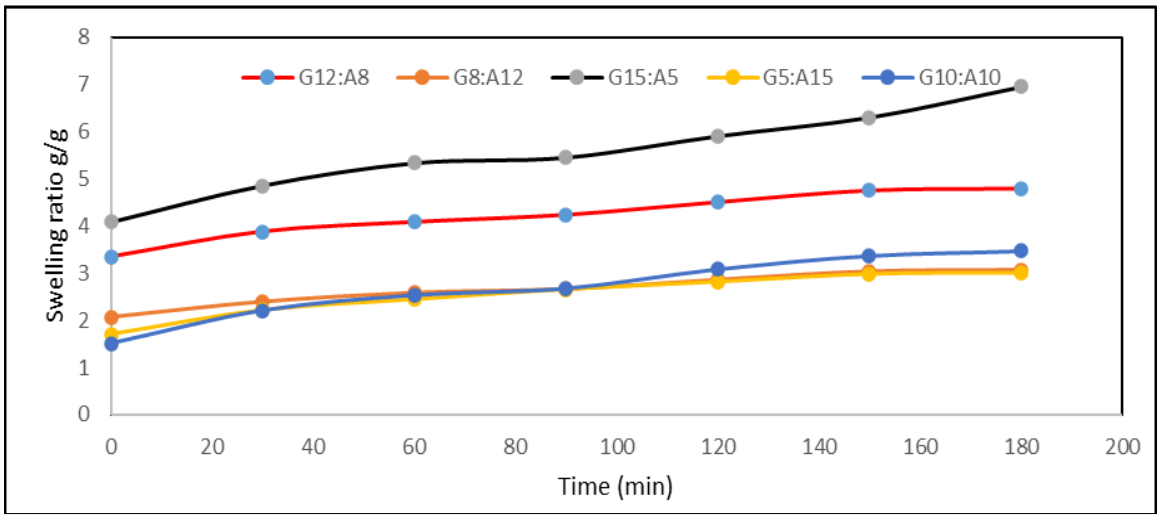


**Fig. 2.** Swelling ratio graph.

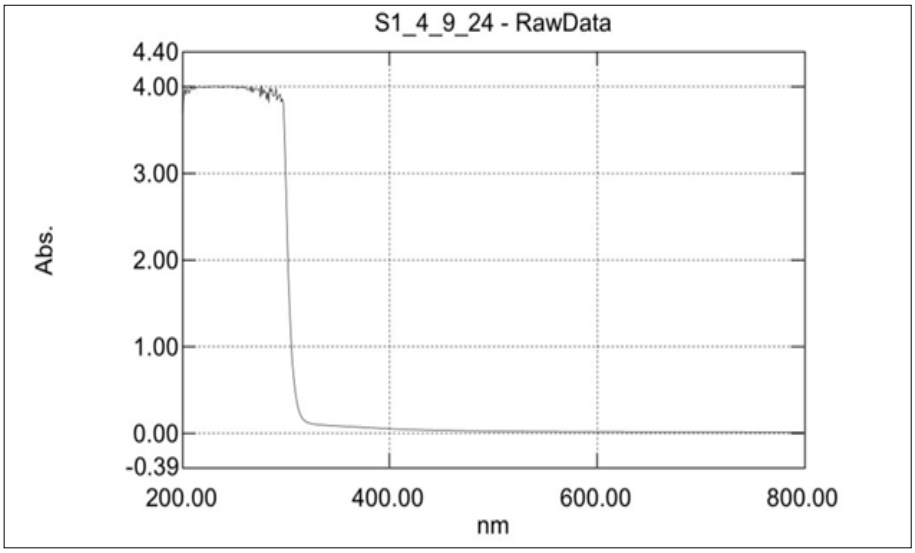


**Fig. 3.** Ultraviolet-visible spectra of L-ascorbic acid.

which may be attributed to aromatic C=C stretching or N-H bending. Gelatin's C-H group bending was found to have a peak with a wavenumber of 1451.60 $cm^{-1}$. The Ether or amines (C-O or C-N stretching) is represented by the peak at 1244.99 $cm^{-1}$. Wavenumber 1081.86 $cm^{-1}$ was identified as the distinctive peak of the C-O stretching vibration (alcohols, ethers and esters). The presence of aromatic or alkenic groups may be indicated by the second peak at 789.80 $cm^{-1}$, which corresponds to C-H bending. Fourier Transform Infrared Spectroscopy was subsequently used to characterise other peaks in the by-product; the results are shown in the figure below. The large peak at 3273 $cm^{-1}$ indicates the hydroxyl group. The additional signal at 2932 $cm^{-1}$, which represents a methyl ($-CH_3$) or methylene ($-CH_2$) group. An additional signal at 1627 $cm^{-1}$ indicates the existence of a carboxylate group (-C=O) or a water molecule (H-O -H bending). Another peak at 1531 $cm^{-1}$ suggests the presence of amide groups, such as N-H bending or C-N stretching, which may be indicative of proteins. Another peak indicates C-H bending of aliphatic hydrocarbons at 1449 $cm^{-1}$. Another signal at 1238 $cm^{-1}$ confirms the presence of agar's glycosidic linkage and indicates C-O-C stretching (Fig. 4) (22, 23).

## Scanning electron microscopy

The topological features of the polymeric gel, such as gelatin and agar, arise from the entanglement and crosslinking of their polymer chains. Gelatin and agar are polymers and polymer blends; the samples' surface morphology and microstructure can be analyzed using SEM. Some essential characteristics of the physical structure and behaviour of the constituent phases of such composites can be discerned from SEM of these mixes. By using the electron beam, scan the surface of the gel (24). The surface morphology and microstructure of the gel will be shown in high-resolution SEM images. To obtain a clear view of the film's microstructure, capture stills at different resolutions. Chemical and physical crosslinking affect the shape of the composite differently. As a rule, cross-linked gels possess a higher degree of density and homogeneity of the structure (Fig. 5).

## Thermogravimetric analysis

A gelatin and agar polymer gel was analyzed thermo-gravimetrically in order to investigate the thermal decomposition profile of the gel. Weight reduction is presented as a percentage to indicate

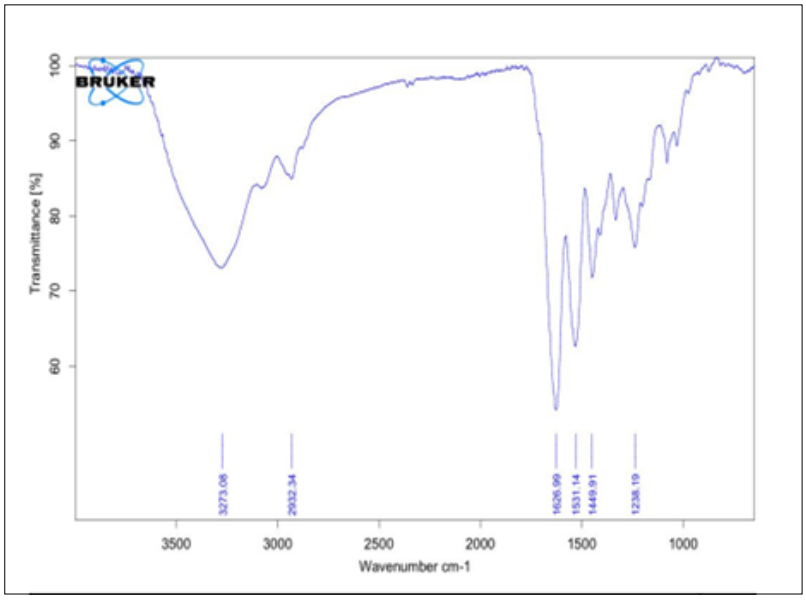


**Fig. 4 (A).** Fourier Transform Infrared Spectroscopy spectra of gelatin gel.

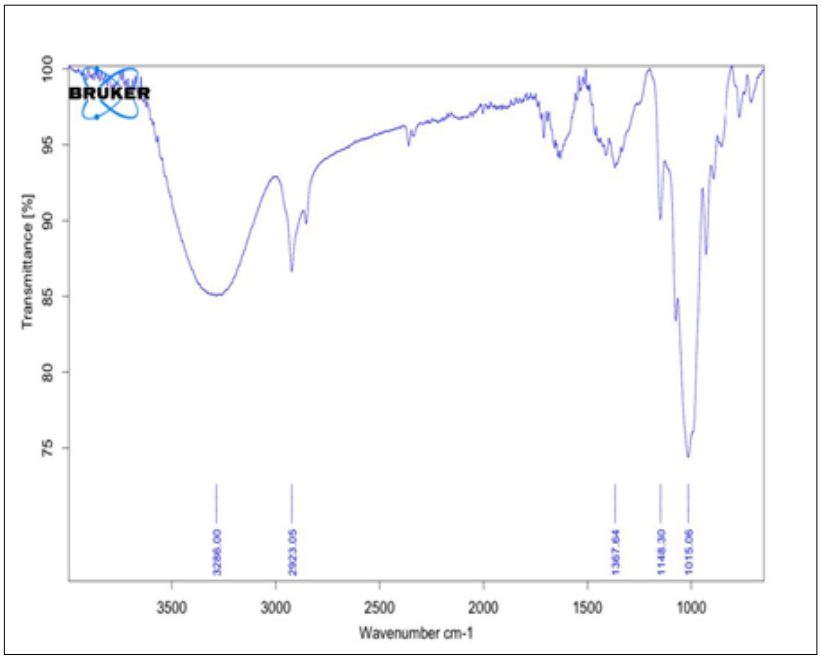


**Fig. 4 (B).** Fourier Transform Infrared Spectroscopy spectra of agar gel.

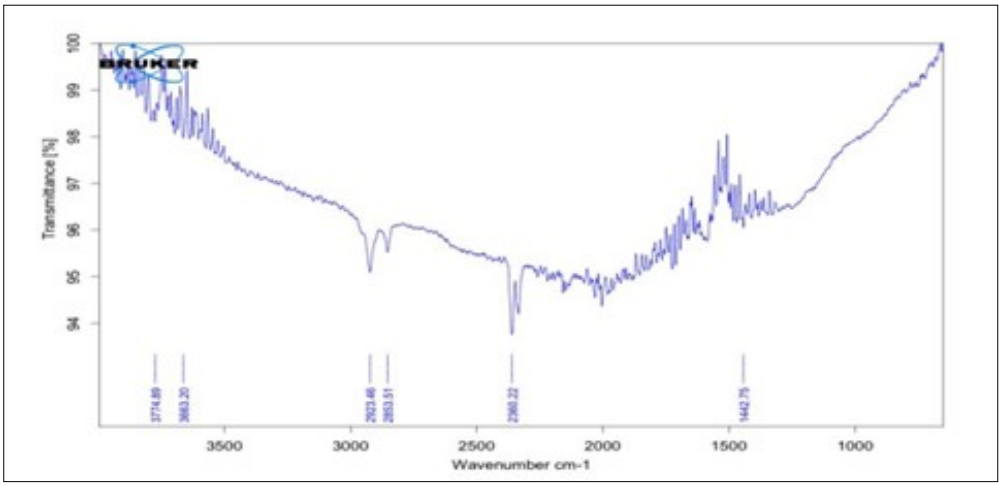


**Fig. 4 (C).** Fourier Transform Infrared Spectroscopy spectra of composite gel.

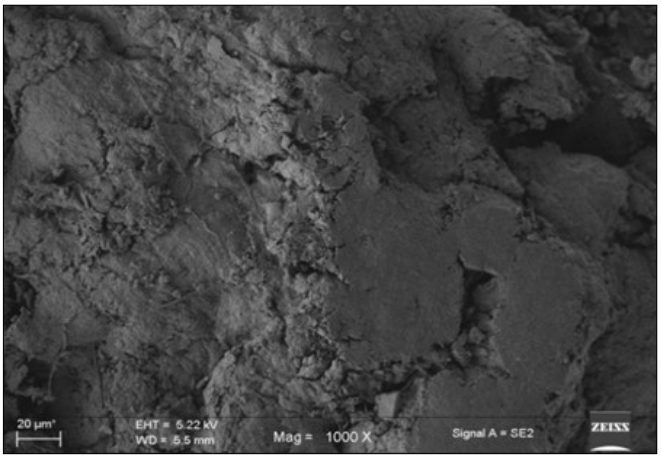


**Fig. 5 (A).** Scanning Electron Microscopic image of composite gel.

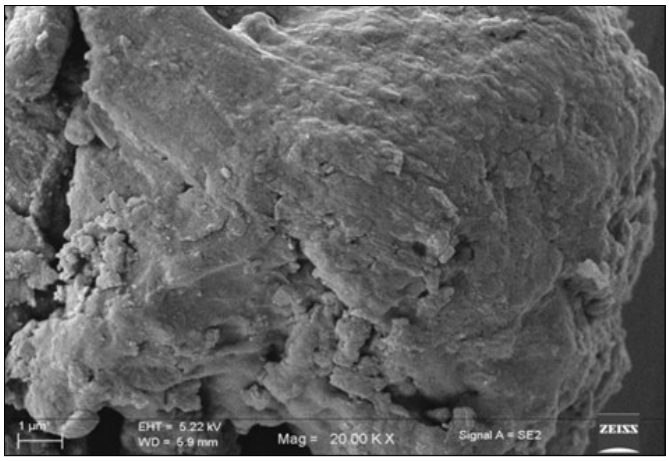


**Fig. 5 (B).** Scanning Electron Microscopic image of composite gel.

achievement. As shown in Fig. 6, an 11.402 mg sample was heated from 25.00 °C to 800.00 °C at a rate of 10.00 °C $min^{-1}$; an initial minor weight loss around 25.08 °C (to 99.803 %) is attributed to moisture loss, followed by a continuous decrease in weight with increasing temperature. As the temperature increased, the sample's weight decreased. When the mean was calculated, it was found at 175.08 °C with a corresponding weight of 85.846 % (25, 26).

## Antibacterial activity

As shown in Fig. 7, antibacterial activity was evaluated using the standard agar disc diffusion method against selected bacterial species, including *Staphylococcus aureus*, to assess the antibacterial drug's efficacy. The drug-loaded composite gel exhibits antibacterial activity, inhibiting bacterial growth after 24 hr of incubation, as

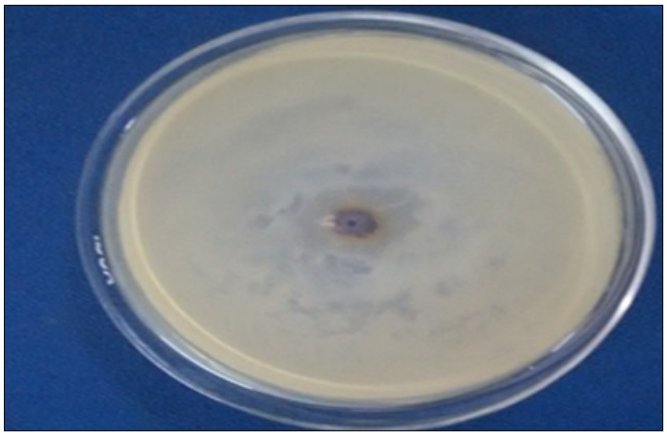

**Fig. 7.** Antibacterial study with zone inhibition study.

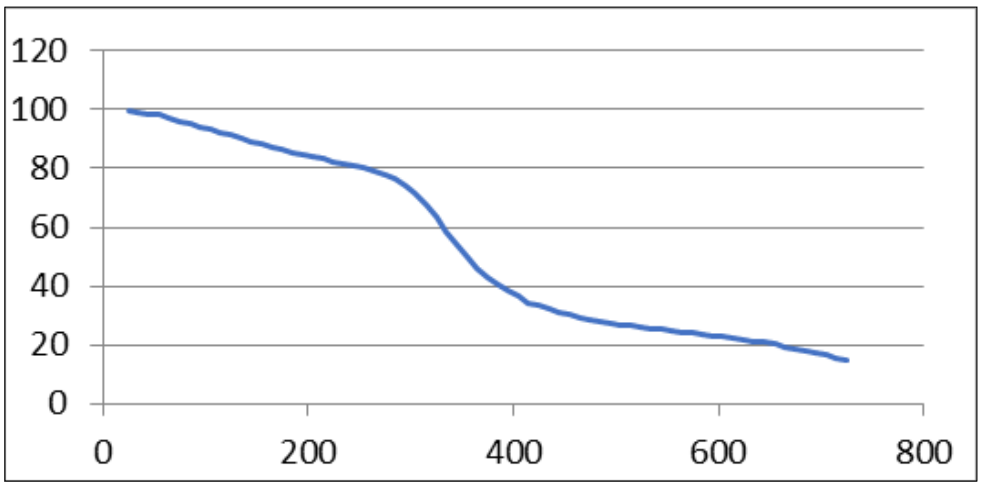


**Fig. 6.** Thermo Gravimetric Analysis graph of composite gel.

measured at approximately 0.5 cm.

## Anti-inflammatory activity

It was observed that when heat-denatured bovine albumin was used in the protein denaturation assay, the protein denaturation and hold steps exerted anti-inflammatory effects. The protein denaturation method, when used to determine the percentage anti-inflammatory effect, showed that the percentage at 1 % allograft inflammatory factor (AIF) increased with increasing drug doses following bovine serum albumin (BSA) denaturation. The newly formed compounds were tested for *in vitro* anti-inflammatory activity using the albumin denaturation method. In this study, we observed the anti-inflammatory activity of the sample at various concentrations, as shown in Fig. 8.

## Dynamic moisture adsorption studies

The dynamic moisture uptake by film samples was examined at 30 ° C with a 95 % relative humidity. The film samples exhibit water vapour sorption curves similar to those observed in polysaccharide-based films (Fig. 9) (13).

## Biocompatibility test

Also, when red blood cells are lysed, the material and other internal components, including Haemoglobin, are released into the surrounding fluid, such as blood plasma. This process is referred to as haemolysis, which may occur naturally during the normal course of red blood cell development or as a result of physical or chemical trauma or underlying pathological conditions. A Haemolysis test was carried out on a gelatin-agar composite gel containing the drug and on a gelatin-agar composite gel without the drug, in fluid, including blood plasma. This process is known as haemolysis. This can occur spontaneously as part of red blood cells' (RBCs') typical life cycle or as a result of physical trauma, chemical exposure, or pathological conditions. A haemolysis test was performed on a gelatin-agar composite gel with drug and on a gelatin-agar composite gel without drug. The haemolysis test is done in a 96-well plate. In this case, the positive control value is 0.086 and the negative control value is 0.26667. It shows that the values 0.086 (positive control) and 0.26667 (negative control) serve as benchmarks for calculating haemolysis caused by the gels and it shows how much RBC destruction is produced by the gel samples relative to the positive and negative controls. The effects of haemolysis are summarized in

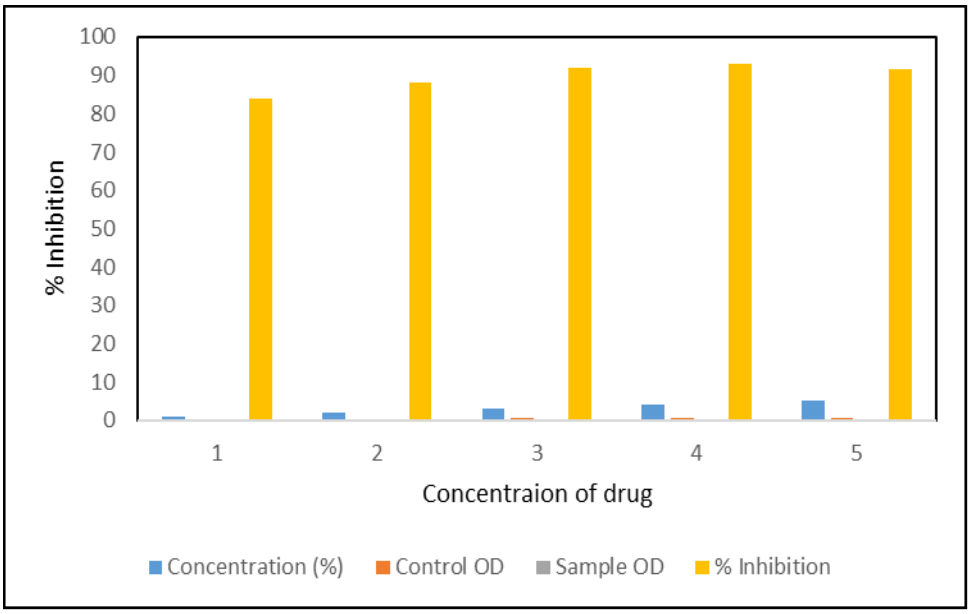


**Fig. 8.** Anti-inflammatory activity with L-ascorbic acid.

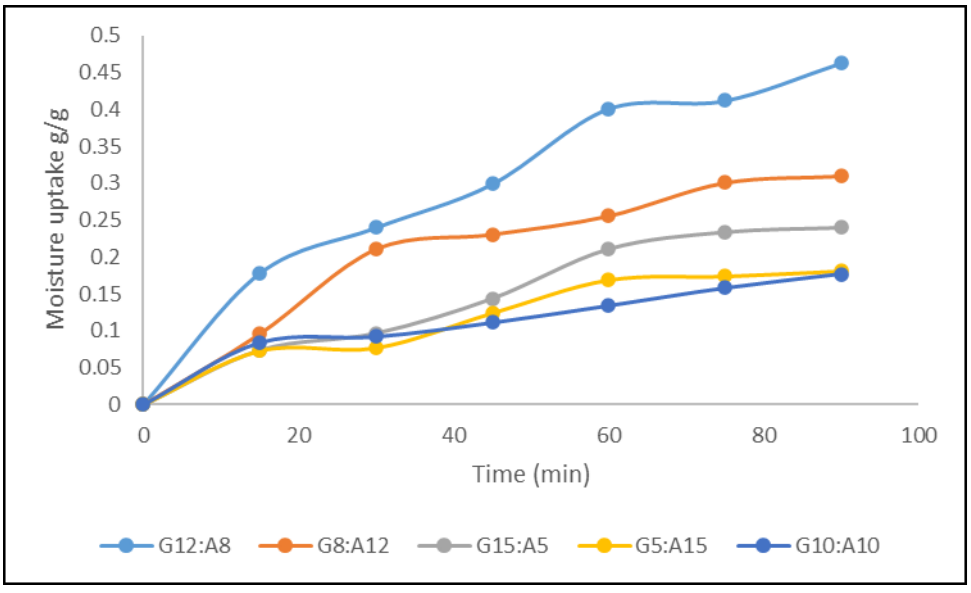


**Fig. 9.** Graph showing moisture uptake.

Table 5 and 6, which present the gel concentrations alongside the corresponding haemolysis percentages (11).

## Conclusion

Thus, the developed gelatin-agar composite hydrogels show great potential for comparing detoxification methods for the foot patch. There is potential for the formation of a sustained-release system when the solubility and stability of agar are enhanced by conjugating it with gelatin, which is biocompatible and biodegradable. The therapeutic potential of L-ascorbic acid-loaded hydrogels for bacterial vaginosis was highlighted by their strong antibacterial activity against Gram-positive and Gram-negative bacteria. Stability, controlled swelling, thermal stability and biocompatibility were among the positive characteristics of the hydrogels; the 15:5 gelatin-agar ratio demonstrated the best swelling capacity. Sterility check, haemolysis, antimicrobials and anti-inflammatory drugs confirmed the efficacy and non-toxicity. Such conclusions recommend further research and clinical utilisation of the hydrogels as potential treatment for bacterial vaginosis and other illnesses.

## Acknowledgements

The authors gratefully acknowledge Parul University, Vadodara for providing access to the FTIR facility. The authors also extend their sincere thanks to PNP Analytical Solution, Vadodara, for their support in conducting the SEM and TGA analysis.

## Authors' contributions

MMIK carried out the synthesis of the hydrogel. SA and VJU participated in the sequence alignment and drafted the manuscript. PJS carried out the synthesis of the drug-loaded hydrogel. BJR participated in the sequence alignment. SYN contributed to the design of the study and performed the swelling study. SR, HSC and NDP performed the characterization. PJD conducted the biocompatibility and antibacterial studies. SA and VJU reviewed the entire manuscript. All authors read and approved the final manuscript.

## Compliance with ethical standards

**Conflict of interest:** The Authors do not have any conflicts of interest to declare.

**Ethical issues:** None

## References

1. Zambroni ME, Bertone PA, Cabral AL, Boatti AS, Romanini SV, Martínez SR, et al. Easy-to-apply hydrogel patch for field treatment and monitoring of equine wounds. Gels. 2025;11:328. https://doi.org/10.3390/gels11050328
2. Tiwari S, Goldmann L, Lübke J, Prucker O, Martin G, Schlunck G, et al. Attachment of hydrogel patches to eye tissue through gel transfer using flexible foils. ACS Appl Mater Interfaces. 2025;17(6):8849–61. https://doi.org/10.1021/acsami.4c15089
3. Zawawi NA, Maarof M, Fadilah NIM, Hao DLQ, Tabata Y, Fauzi MB. Hybrid adhesive hydrogel patch containing genipin-crosslinked gelatin-hyaluronic acid for future use in atopic dermatitis. J Funct Biomater. 2025;16:195. https://doi.org/10.3390/jfb16060195
4. Ahuja S, Fidai RA. Fabrication of copper nano/honey loaded polymeric composite with microbial activity. Res J Pharm Technol. 2023;16(11):5400–405. https://doi.org/10.52711/0974-360X.2023.00874
5. Ahuja S, Sinojia A. Versatile application of polymeric gel using gelatin polymer. Res J Pharm Technol. 2024;17(4):1559–64. https://doi.org/10.52711/0974-360X.2024.00246
6. Ross KA, Pyrak-Nolte LJ, Campanella OH. The effect of mixing conditions on the material properties of an agar gel-microstructural and macrostructural considerations. Food Hydrocoll. 2006;20(1):79–87. https://doi.org/10.1016/j.foodhyd.2005.01.007
7. Singh VK, Sagiri SS, Pal K, Khade SM, Pradhan DK, Bhattacharya MK. Gelatin-carbohydrate phase-separated hydrogels as bioactive carriers in vaginal delivery: Preparation and physical characterizations. J Appl Polym Sci. 2014;131:40445. https://doi.org/10.1002/app.40445
8. Firoozmand H, Rousseau D. Microstructure and elastic modulus of phase-separated gelatin–starch hydrogels containing dispersed oil droplets. Food Hydrocoll. 2013;30(1):333–42. https://doi.org/10.1016/j.foodhyd.2012.06.010
9. Echave MC, Sánchez P, Pedraz JL, Orive G. Progress of gelatin-based 3D approaches for bone regeneration. J Drug Deliv Sci Technol. 2017;41:292–302. https://doi.org/10.1016/j.jddst.2017.04.012
10. Hill E, Boontheekul T, Mooney DJ. Designing scaffolds to enhance transplanted myoblast survival and migration. Tissue Eng. 2006;12(5):1295–304. https://doi.org/10.1089/ten.2006.12.1295
11. Bajpai SK, Chand N, Ahuja S, Roy MK. Curcumin/cellulose microcrystals/chitosan films: Water absorption behavior and *in vitro* cytotoxicity. Int J Biol Macromol. 2015;75:239–47. https://doi.org/10.1016/j.ijbiomac.2015.01.038
12. Bajpai SK, Daheriya P, Ahuja S, Gupta K. Water absorption and antimicrobial behavior of physically cross-linked poly(vinyl alcohol)/carrageenan films loaded with minocycline. Des Monomers Polym. 2016;19(7):630–42. https://doi.org/10.1080/15685551.2016.1187444
13. Bajpai SK, Chand N, Ahuja S, Roy MK. Vapor-induced phase inversion technique to prepare chitosan/microcrystalline cellulose composite films: Synthesis, characterization and moisture absorption study. Cellulose. 2015;22(6):3825–37. https://doi.org/10.1007/s10570-015-0775-z
14. Allo JD, Pakan PD, Setiawan IMB, Iswaningsih. Formulation and antibacterial test of *Moringa oleifera* seed extract gel preparations on *Staphylococcus aureus*. Int J Drug Deliv Technol. 2025;15(1):86–90. https://doi.org/10.25258/ijddt.15.1.11
15. Kondapure AA, Koumaravelou K. Antiinflammatory activity of *Arquita ancashiana* nanoemulgel: *in vitro* and *in vivo* evaluation. Int J Drug Deliv Technol. 2025;15(1):271–78. https://doi.org/10.25258/ijddt.15.1.38
16. Patil AR, Maru AD. Phytochemical characterization and evaluation of antioxidant, antiinflammatory, antibacterial and antifungal activities of *Nigella sativa*-based nanoemulgel (NEGIS). Int J Drug Deliv Technol. 2025;15(1):230–37. https://doi.org/10.25258/ijddt.15.1.32
17. Bajpai SK, Chand N, Ahuja S, Roy MK. Investigation of curcumin release from chitosan/cellulose microcrystals (CMC) antimicrobial films. Int J Biol Macromol. 2015;79:440–48. https://doi.org/10.1016/j.ijbiomac.2015.05.012
18. Bajpai SK, Ahuja S, Chand N, Bajpai M. Nanocellulose-dispersed chitosan film with Ag NPs/curcumin: An *in vivo* study on albino rats for wound dressing. Int J Biol Macromol. 2017;104:1012–19. https://doi.org/10.1016/j.ijbiomac.2017.06.096
19. Pal K, Banthia AK, Majumdar DK. Preparation and characterization of polyvinyl alcohol–gelatin hydrogel membranes for biomedical applications. AAPS PharmSciTech. 2007;8(1):142–46. https://doi.org/10.1208/pt080121
20. Pourjavadi A, Farhadpour B, Seidi FS. Synthesis and investigation of

swelling behavior of new agar-based superabsorbent hydrogel as a candidate for agrochemical delivery. J Polym Res. 2009;16(6):655–65. https://doi.org/10.1007/s10965-009-9270-2

21. Yang H, Irudayaraj J, Paradkar MM. Discriminant analysis of edible oils and fats by FTIR, FT-NIR and FT-Raman spectroscopy. Food Chem. 2005;93(1):25–32. https://doi.org/10.1016/j.foodchem.2004.08.039
22. Bajpai SK, Ahuja S, Daheriya P, Bajpai M. A green approach to prepare Ag NPs-loaded IC/PVA polymeric film for antimicrobial applications. J Macromol Sci A. 2017;54(11):835–42. https://doi.org/10.1080/10601325.2017.1337470
23. Shiinoki Y, Yano T. Viscoelastic behavior of an agar–gelatin mixture gel as a function of its composition. Food Hydrocoll. 1986;1(2):153–61.
24. Atole DM, Rajput HH. Ultraviolet spectroscopy and its pharmaceutical applications-A brief review. Asian J Pharm Clin Res. 2017;11(2):59–63. https://doi.org/10.1016/j.fpsl.2020.100583
25. Najwa INA, Guerrero P, de la Caba K, Hanani ZN. Physical and antioxidant properties of starch/gelatin films incorporated with *Garcinia atroviridis* leaves. Food Packag Shelf Life. 2020;26:100583. https://doi.org/10.1016/j.fpsl.2020.100583
26. Fang CC, Zhang Y, Qi SY, Liao YC, Li YY, Wang P. Influence of structural design on mechanical and thermal properties of jute-reinforced polylactic acid (PLA) laminated composites. Cellulose. 2020;27:9397–407. https://doi.org/10.1007/s10570-020-03436-8

## Additional information

**Peer review**: Publisher thanks Sectional Editor and the other anonymous reviewers for their contribution to the peer review of this work.

**Reprints & permissions information** is available at https://horizonepublishing.com/journals/index.php/PST/open_access_policy

**Publisher's Note**: Horizon e-Publishing Group remains neutral with regard to jurisdictional claims in published maps and institutional affiliations.

**Indexing**: Plant Science Today, published by Horizon e-Publishing Group, is covered by Scopus, Web of Science, BIOSIS Previews, Clarivate Analytics, NAAS, UGC Care, etc
See https://horizonepublishing.com/journals/index.php/PST/indexing_abstracting



**Publisher information:** Plant Science Today is published by HORIZON e-Publishing Group with support from Empirion Publishers Private Limited, Thiruvananthapuram, India.